IEICE TRANS. FUNDAMENTALS, VOL.E106–A, NO.10 OCTOBER 2023

PAPER

Bayesian Learning-Assisted Joint Frequency Tracking and Channel Estimation for OFDM Systems

Hong-Yu LIU[†a)], ***Nonmember***

SUMMARY Orthogonal frequency division multiplexing (OFDM) is very sensitive to the carrier frequency offset (CFO). The CFO estimation precision heavily makes impacts on the OFDM performance. In this paper, a new Bayesian learning-assisted joint CFO tracking and channel impulse response estimation is proposed. The proposed algorithm is modified from a Bayesian learning-assisted estimation (BLAE) algorithm in the literature. The BLAE is expectation-maximization (EM)-based and displays the estimator mean square error (MSE) lower than the Cramer-Rao bound (CRB) when the CFO value is near zero. However, its MSE value may increase quickly as the CFO value goes away from zero. Hence, the CFO estimator of the BLAE is replaced to solve the problem. Originally, the design criterion of the single-time-sample (STS) CFO estimator in the literature is maximum likelihood (ML)-based. Its MSE performance can reach the CRB. Also, its CFO estimation range can reach the widest range required for a CFO tracking estimator. For a CFO normalized by the sub-carrier spacing, the widest tracking range required is from −0.5 to +0.5. Here, we apply the STS CFO estimator design method to the EM-based Bayesian learning framework. The resultant Bayesian learning-assisted STS algorithm displays the MSE performance lower than the CRB, and its CFO estimation range is between ±0.5. With such a Bayesian learning design criterion, the additional channel noise power and power delay profile must be estimated, as compared with the ML-based design criterion. With the additional channel statistical information, the derived algorithm presents the MSE performance better than the CRB. Two frequency-selective channels are adopted for computer simulations. One has fixed tap weights, and the other is Rayleigh fading. Comparisons with the most related algorithms are also been provided.

key words: *orthogonal frequency division multiplexing, carrier frequency offset, channel estimation, Cramer-Rao bound, Bayesian learning*

1. Introduction

Orthogonal frequency division multiplexing (OFDM) is very sensitive to the carrier frequency offset (CFO), which arises from the Doppler shift and/or the mismatch between the transmitter and the receiver oscillators [1]. The CFO can heavily degrade the system performance, and there have been many research reports on the CFO estimation, e.g., [2]–[4] and references therein.

To gain high estimation precision, the maximum likelihood (ML)-based algorithms are the most popular [2]–[4]. For the joint CFO tracking and channel impulse response (CIR) estimation, an ML CIR estimator is certainly the choice, e.g., [5]–[10] and references therein. As for the CFO estimator design, there have been various ML-based design methods as discussed below. In [5], the conventional steepest-descent method was used for the CFO estimator. In [6]–[9], to make mathematical tractability, the Taylor approximations were made by taking the Taylor series truncated to finite orders for the CFO estimator design. In particular, by the order-recursive [8] or the high-order [9] Taylor approximation, the widest CFO estimation range required for a CFO tracking estimator can be reached. For a CFO normalized by the sub-carrier spacing, the widest tracking range required is from −0.5 to +0.5 [4]. However, their computational complexities are quite large. In [10], instead of directly using the whole received signal block as the above mentioned [5]–[9], the authors first designed a set of crude ML CFO estimators based on each single-time-slot sample. Then, these crude CFO estimators were linearly combined in the minimum mean square error (MMSE) sense to obtain a more accurate CFO estimator, called the single-time-sample (STS) ML CFO estimator. The CFO estimation range of the STS-ML CFO estimator can reach between −0.5 and +0.5 without resorting to the order-recursive [8] or the high-order [9] Taylor approximation. Thus, the high computational complexity is avoided. By the way, for brevity, the joint CFO tracking and CIR estimation algorithm reported in [10] is called the STS-ML algorithm in this paper.

One thing must be made clear that there are two versions, Version A and Version B, were presented for the STS-ML algorithms in [10]. In this paper, the STS-ML algorithm is specifically referred to the Version B algorithm because it is the most related to our proposed algorithm.

Next, the optimal mean square error (MSE) performance for the ML-based algorithms, e.g., [5]–[10] and references therein, is the Cramer-Rao bound (CRB) [11]. To acquire the MSE performance lower than the CRB, we must resort to other design criterions. It is well known that an MMSE CIR estimator displays better MSE than an ML CIR estimator [12]. Therefore, we focus on the joint CFO tracking and MMSE CIR estimation in this paper.

An MMSE CIR estimate can be seen as a weighted ML CIR estimate [12]. The additional channel noise power (CNP) and the power delay profile (PDP) must be provided for those weighting factors in an MMSE CIR estimator. Therefore, the computational complexity of an MMSE CIR estimator is higher than that of an ML CIR estimator. Fortunately, the incremental complexity is moderate when a preamble sequence with constant amplitude is adopted.

Assisted by the expectation-maximization (EM) algo-

Manuscript received December 26, 2022.
Manuscript revised February 19, 2023.
Manuscript publicized March 30, 2023.

[†]The author is with Fu Jen Catholic University, New Taipei City 24205, Taiwan.
a) E-mail: 087676@mail.fju.edu.tw

DOI: 10.1587/transfun.2022EAP1167

rithm, the joint CFO tracking and CIR estimation algorithms developed in [13]–[16] adopt the MMSE CIR. However, in [13] and [14], the MMSE CIR estimators are approximated by the ML CIR estimators for complexity reduction. In [15], the CNP and PDP are assumed having been perfectly estimated. Only the Bayesian learning-assisted estimation (BLAE) algorithm developed in [16] takes the CNP estimator and the PDP estimator into account. The weakness of the BLAE is that its CFO estimation range is very small.

In this paper, a Bayesian learning-assisted STS (BLASTS) algorithm for the joint CFO tracking and CIR estimation will be proposed. We will replace the CFO estimator of the BLAE with that of the STS-ML. The choice of the CIR estimator in the BLAE is due to the fact that its CIR estimator is optimal in the MMSE sense. In addition, the choice of the CFO estimator in the STS-ML lies on its wide CFO estimation range. Notice that the resultant STS CFO estimator is an EM-based CFO estimator instead of an ML-based one as presented in [10]. In brief, the proposed BLASTS is a joint MMSE CIR and STS CFO estimation. It turns out that the BLASTS consists of an MMSE CIR estimator, a CNP estimator, a PDP estimator and an STS CFO estimator. The computer simulations comparing the BLASTS with the BLAE and the STS-ML will also be provided.

2. System Model

Consider an OFDM system with N sub-carriers. Its n th sub-carrier information symbol X_n is placed at the n th diagonal entry of the diagonal matrix $\boldsymbol{U}_X = \text{Diag}\{X_0, X_1, \cdots, X_{N-1}\}$. The column vector $\boldsymbol{h}$ of size L denotes the CIR and is a circularly symmetric complex Gaussian random vector with mean vector $\boldsymbol{0}_L$ and covariance matrix $\boldsymbol{C}_h = \text{Diag}\{\lambda_0, \lambda_1, \cdots, \lambda_{L-1}\}$, where $\boldsymbol{0}_L$ stands for an all-zero column vector of size L. The Gaussian random vector can also be denoted as $CN(\boldsymbol{0}_L, \boldsymbol{C}_h)$. The column vector $\boldsymbol{w}$ of size N represents the channel noise vector and is modeled as $CN(\boldsymbol{0}_N, \rho\boldsymbol{I}_N)$, where $\boldsymbol{I}_N$ stands for the identity matrix of size N. $\boldsymbol{F}_N$ stands for the N-point discrete Fourier transform (DFT) matrix with the (m,n)th entry being $e^{-j2\pi mn/N}$ for $m \in \{0, 1, \cdots, N-1\}$ and $n \in \{0, 1, \cdots, N-1\}$. Then, we define $\boldsymbol{F}_L$ as the first L column vectors of $\boldsymbol{F}_N$. The CFO normalized by the sub-carrier spacing is denoted by δ, which is unitless because of taking the normalization. For a CFO tracking problem, δ may be between -0.5 and $+0.5$.

After the removal of the cyclic prefix, the received signal vector is given by

$$\boldsymbol{r} = \boldsymbol{D}_\delta \boldsymbol{A}\boldsymbol{h} + \boldsymbol{w}, \tag{1}$$

where $\boldsymbol{D}_\delta = \text{Diag}\left\{e^{j2\pi 0\cdot\frac{\delta}{N}}, e^{j2\pi 1\cdot\frac{\delta}{N}}, \cdots, e^{j2\pi(N-1)\cdot\frac{\delta}{N}}\right\}$ and $\boldsymbol{A} = \boldsymbol{F}_N^H \boldsymbol{U}_X \boldsymbol{F}_L / N$ with the superscript H denoting the Hermitian transpose. The nth time-slot sample r_n of $\boldsymbol{r} = [r_0, r_1, \cdots, r_{N-1}]^T$ with the superscript T denoting the transpose is given by

$$r_n = e^{j2\pi n\delta/N} \boldsymbol{a}_n^T \boldsymbol{h} + w_n, \tag{2}$$

where $\boldsymbol{a}_n^T$ is the nth row vector of $\boldsymbol{A} = [\boldsymbol{a}_0, \boldsymbol{a}_1, \cdots, \boldsymbol{a}_{N-1}]^T$, and w_n represents the nth entry of $\boldsymbol{w} = [w_0, w_1, \cdots, w_{N-1}]^T$.

Taking the logarithm on the joint probability density function (PDF) $p(\boldsymbol{r}, \boldsymbol{h})$ of the received signal $\boldsymbol{r}$ and the CIR $\boldsymbol{h}$, we can obtain [11]

$$\begin{aligned} \ln p(\boldsymbol{r}, \boldsymbol{h}) &= \ln p(\boldsymbol{h}) + \ln p(\boldsymbol{r}|\boldsymbol{h}) \\ &= -L\ln\pi - \sum_{l=0}^{L-1} \ln\lambda_l - \boldsymbol{h}^H \boldsymbol{C}_h^{-1} \boldsymbol{h} \\ &\quad - N\ln(\pi\rho) - |\boldsymbol{r} - \boldsymbol{D}_\delta \boldsymbol{A}\boldsymbol{h}|^2 / \rho. \end{aligned} \tag{3}$$

Then, taking the logarithm on the joint PDF $p(r_n, \boldsymbol{h})$ of the received nth time-slot sample r_n of $\boldsymbol{r}$ and the CIR $\boldsymbol{h}$, we can obtain

$$\begin{aligned} \ln p(r_n, \boldsymbol{h}) &= \ln p(\boldsymbol{h}) + \ln p(r_n|\boldsymbol{h}) \\ &= -L\ln\pi - \sum_{l=0}^{L-1} \ln\lambda_l - \boldsymbol{h}^H \boldsymbol{C}_h^{-1} \boldsymbol{h} \\ &\quad - \ln(\pi\rho) - \left|r_n - e^{j2\pi n\delta/N} \boldsymbol{a}_n^T \boldsymbol{h}\right|^2 / \rho. \end{aligned} \tag{4}$$

3. BLASTS Algorithm Derivation

The CIR estimator and the PDP estimator are the same as those in [16] without any modifications. They are briefly reviewed first and are followed by the CNP estimator. The CNP estimator is largely the same as that in [16] except for a slight modification to its expression. Then, the detailed derivation process for the EM-based STS CFO estimator is described. Finally, the BLASTS algorithm is provided.

3.1 CIR Estimator and PDP Estimator

The CIR estimator is the mean of $\boldsymbol{h}$ conditioned on $\boldsymbol{r}$, given by [16, Eq. (10)]

$$\text{E}_{h|r}\{\boldsymbol{h}\} = \boldsymbol{\mu}_{h|r} = \left(\boldsymbol{C}_h^{-1}\rho + \boldsymbol{A}^H\boldsymbol{A}\right)^{-1} \boldsymbol{A}^H \boldsymbol{D}_\delta^H \boldsymbol{r}, \tag{5}$$

where $\text{E}_{h|r}\{\ \ \}$ denotes taking the expectation with respect to $\boldsymbol{h}$ conditioned on $\boldsymbol{r}$ and $\boldsymbol{\mu}_{h|r}$ is the brief notation for $\text{E}_{h|r}\{\boldsymbol{h}\}$ for later use. In fact, the CIR estimator of (5) is equivalent to an MMSE CIR estimator [11, Ch. 12].

Based on the EM algorithm displayed in [16], the PDP estimator maximizes $\text{E}_{h|r}\{\ln p(\boldsymbol{r}, \boldsymbol{h})\}$. By setting the derivative of $\text{E}_{h|r}\{\ln p(\boldsymbol{r}, \boldsymbol{h})\}$ with respect to λ_l to zero, the PDP estimator can be obtained as [16, Eq. (15)]

$$\lambda_l = [\boldsymbol{C}_{h|r}]_{l,l} + \left|[\boldsymbol{\mu}_{h|r}]_l\right|^2, \tag{6}$$

where

$$\boldsymbol{C}_{h|r} = \rho\left(\boldsymbol{C}_h^{-1}\rho + \boldsymbol{A}^H\boldsymbol{A}\right)^{-1} \tag{7}$$

is the covariance matrix of $\boldsymbol{h}$ conditioned on $\boldsymbol{r}$, $[\ ]_{l,l}$ denotes the (l,l)th entry of the matrix inside the brackets, $[\ ]_l$ is the lth entry of the vector inside the brackets, and

$l \in \{0, 1, \cdots, L-1\}$.

3.2 CNP Estimator

The CNP estimator based on the EM algorithm displayed in [16] also maximizes $\mathrm{E}_{h|r}\{\ln p(\boldsymbol{r}, \boldsymbol{h})\}$. By setting the derivative of $\mathrm{E}_{h|r}\{\ln p(\boldsymbol{r}, \boldsymbol{h})\}$ with respect to ρ to zero, the CNP estimator can be expressed as [16, Eq. (18)]

$$\begin{aligned}\rho_{(i)} &= \frac{1}{N}\left[|\boldsymbol{r}|^2 - 2\mathrm{Re}\left\{\boldsymbol{r}^H \boldsymbol{D}_\delta \boldsymbol{A}\boldsymbol{\mu}_{h|r}\right\} + \rho_{(i-1)}\right. \\ &\quad \left.\cdot \mathrm{Tr}\left\{\left(\boldsymbol{C}^{-1}_{h|r,(i)} - \boldsymbol{C}^{-1}_{h,(i-1)}\right)\left(\boldsymbol{C}_{h|r,(i)} + \boldsymbol{\mu}_{h|r}\boldsymbol{\mu}^H_{h|r}\right)\right\}\right] \\ &= \frac{1}{N}\left[|\boldsymbol{r}|^2 - 2\boldsymbol{r}^H \boldsymbol{D}_\delta \boldsymbol{A}\boldsymbol{\mu}_{h|r}\right. \\ &\quad \left. + \mathrm{Tr}\left\{\boldsymbol{A}^H \boldsymbol{A}\left(\boldsymbol{C}_{h|r,(i)} + \boldsymbol{\mu}_{h|r}\boldsymbol{\mu}^H_{h|r}\right)\right\}\right], \end{aligned} \tag{8}$$

where each additional subscript (i) denotes the ith iteration in an iterative adaption process, and, to arrive at the 2nd equality of (8), the property that $\boldsymbol{r}^H \boldsymbol{D}_\delta \boldsymbol{A}\boldsymbol{\mu}_{h|r}$ is real and the equality $\rho_{(i-1)}(\boldsymbol{C}^{-1}_{h|r,(i)} - \boldsymbol{C}^{-1}_{h,(i-1)}) = \boldsymbol{A}^H\boldsymbol{A}$ [16, Eq. (A.2)] have been used. It can be readily found that the Hermitian of $\boldsymbol{r}^H \boldsymbol{D}_\delta \boldsymbol{A}\boldsymbol{\mu}_{h|r}$ goes back to itself by substituting $\boldsymbol{\mu}_{h|r}$ of (5) into $\boldsymbol{r}^H \boldsymbol{D}_\delta \boldsymbol{A}\boldsymbol{\mu}_{h|r}$. Therefore, that $\boldsymbol{r}^H \boldsymbol{D}_\delta \boldsymbol{A}\boldsymbol{\mu}_{h|r}$ is real has been proved. Notice that the CNP estimator in [16] adopts the 1st equality of (8) whereas the CNP estimator chosen in this paper adopts the 2nd equality of (8). The reason for choosing the 2nd equality of (8) is that $\boldsymbol{A}^H\boldsymbol{A}$ is a constant matrix known to the receiver. However, the values of $\boldsymbol{C}_{h|r,(i)}$ and $\boldsymbol{C}_{h,(i-1)}$ are unreliable before the iteration process converges.

3.3 STS CFO Estimator

Instead of maximizing $\mathrm{E}_{h|r}\{\ln p(\boldsymbol{r}, \boldsymbol{h})\}$ for the CFO estimator design adopted in [16], we maximize $\mathrm{E}_{h|r}\{\ln p(r_n, \boldsymbol{h})\}$ first for developing a set of crude CFO estimators. Then, we linearly combined these crude CFO estimators in the MMSE sense, leading to a more accurate CFO estimator.

By setting the derivative of $\mathrm{E}_{h|r}\{\ln p(r_n, \boldsymbol{h})\}$ with respect to δ to zero, the result is

$$\mathrm{Im}\left\{r_n^* e^{j2\pi n\delta/N} \boldsymbol{a}_n^T \boldsymbol{\mu}_{h|r}\right\} = 0, \tag{9}$$

where Im{ } represents taking the imaginary part. Furthermore, we define $\hat{\delta}_n$ as the nth STS CFO estimate of δ. Then, the solution to (9) can be expressed as

$$\hat{\delta}_n = \frac{N}{2\pi n}\mathrm{Arg}\left\{r_n\left(\boldsymbol{a}_n^T\boldsymbol{\mu}_{h|r}\right)^*\right\}, \tag{10}$$

where Arg{ } is the angle of the complex number in the braces and $\hat{\delta}_0 = 0$ since r_0 contains no CFO.

Let the estimation error of $\hat{\delta}_n$ be $\Delta\hat{\delta}_n = \hat{\delta}_n - \delta$. Then,

$$\begin{aligned}\Delta\hat{\delta}_n &= \frac{N}{2\pi n}\mathrm{Arg}\left\{r_n\left(\boldsymbol{a}_n^T\boldsymbol{\mu}_{h|r}\right)^* e^{-j2\pi n\delta/N}\right\} \\ &= \frac{N}{2\pi n}\frac{\mathrm{Im}\{w_n\left(\boldsymbol{a}_n^T\boldsymbol{\mu}_{h|r}\right)^* e^{-j2\pi n\delta/N}\}}{\left|\boldsymbol{a}_n^T\boldsymbol{\mu}_{h|r}\right|^2}, \end{aligned} \tag{11}$$

where the small $\Delta\hat{\delta}_n$ assumption, i.e.,

$$\mathrm{Arg}\left\{r_n\left(\boldsymbol{a}_n^T\boldsymbol{\mu}_{h|r}\right)^* e^{-\frac{j2\pi n\delta}{N}}\right\} \approx \frac{\mathrm{Im}\{r_n\left(\boldsymbol{a}_n^T\boldsymbol{\mu}_{h|r}\right)^* e^{-j2\pi n\delta/N}\}}{\mathrm{Re}\left\{r_n\left(\boldsymbol{a}_n^T\boldsymbol{\mu}_{h|r}\right)^* e^{-j2\pi n\delta/N}\right\}} \tag{12}$$

with Re{ } representing taking the real part, and the high signal-to-noise ratio (SNR) have been used to reach the 2nd equality of (11). Furthermore, the MSE of $\hat{\delta}_n$ can be obtained as

$$\mathrm{E}_w\left\{\left(\Delta\hat{\delta}_n\right)^2\right\} = \frac{N^2\rho}{8\pi^2 n^2\left|\boldsymbol{a}_n^T\boldsymbol{\mu}_{h|r}\right|^2}, \tag{13}$$

where $\mathrm{E}_w\{\ \}$ denotes taking the expectation with respect to $\boldsymbol{w}$, and $\mathrm{E}_w\left\{\boldsymbol{w}\boldsymbol{w}^H\right\} = \rho\boldsymbol{I}_N$ and $\mathrm{E}_w\left\{\boldsymbol{w}\boldsymbol{w}^T\right\} = \boldsymbol{0}_{N,N}$, with $\boldsymbol{0}_{N,N}$ representing the all-zero $N \times N$ matrix, have been used to arrive at (13).

To proceed, the proposed CFO estimator is constructed by linearly combined those crude CFO estimators, given by $\hat{\delta} = \sum_{n=1}^{N-1}\alpha_n\hat{\delta}_n$ with $\sum_{n=1}^{N-1}\alpha_n = 1$. Next, define the estimation error of the proposed CFO estimator as $\Delta\hat{\delta} = \hat{\delta} - \delta$. Then, the weights $\{\alpha_n\}$ are determined by minimizing the MSE

$$\mathrm{E}_w\left\{\left(\Delta\hat{\delta}\right)^2\right\} = \sum_{n=1}^{N-1}\alpha_n^2\frac{N^2\rho}{8\pi^2 n^2\left|\boldsymbol{a}_n^T\boldsymbol{\mu}_{h|r}\right|^2} \tag{14}$$

subject to $\sum_{n=1}^{N-1}\alpha_n = 1$. By employing the Lagrange method [17], the solution for α_n can be expressed as

$$\alpha_n = \frac{n^2\left|\boldsymbol{a}_n^T\boldsymbol{\mu}_{h|r}\right|^2}{\boldsymbol{\mu}^H_{h|r}\boldsymbol{A}^H\boldsymbol{Q}_N^2\boldsymbol{A}\boldsymbol{\mu}_{h|r}} \tag{15}$$

with $\boldsymbol{Q}_N = \mathrm{Diag}\{0, 1, \cdots, N-1\}$. Accordingly, the proposed CFO estimator is given by

$$\hat{\delta} = \sum_{n=1}^{N-1}\alpha_n\hat{\delta}_n = \frac{\boldsymbol{\mu}^H_{h|r}\boldsymbol{A}^H\boldsymbol{Q}_N^2\boldsymbol{\Gamma}\boldsymbol{A}\boldsymbol{\mu}_{h|r}}{\boldsymbol{\mu}^H_{h|r}\boldsymbol{A}^H\boldsymbol{Q}_N^2\boldsymbol{A}\boldsymbol{\mu}_{h|r}} \tag{16}$$

with $\boldsymbol{\Gamma} = \mathrm{Diag}\left\{\hat{\delta}_0, \hat{\delta}_1, \cdots, \hat{\delta}_{N-1}\right\}$.

In an iterative adaption process, we reconsider the role that $\hat{\delta}$ of (16) represents. At the ith iteration, $\hat{\delta}$ of (16) is redefined as the difference $\Delta\hat{\delta}_{(i)}$ between present estimate $\hat{\delta}_{(i)}$ and the previous estimate $\hat{\delta}_{(i-1)}$, i.e.,

$$\Delta\hat{\delta}_{(i)} = \hat{\delta}_{(i)} - \hat{\delta}_{(i-1)}, \tag{17}$$

Hence, we rewrite (16) as

$$\Delta\hat{\delta}_{(i)} = \frac{\boldsymbol{\mu}^H_{h|r}\boldsymbol{A}^H\boldsymbol{Q}_N^2\Delta\boldsymbol{\Gamma}_{(i)}\boldsymbol{A}\boldsymbol{\mu}_{h|r}}{\boldsymbol{\mu}^H_{h|r}\boldsymbol{A}^H\boldsymbol{Q}_N^2\boldsymbol{A}\boldsymbol{\mu}_{h|r}}, \tag{18}$$

with

$$\Delta\boldsymbol{\Gamma}_{(i)} = \mathrm{Diag}\left\{\Delta\hat{\delta}_{0,(i)}, \Delta\hat{\delta}_{1,(i)}, \cdots, \Delta\hat{\delta}_{N-1,(i)}\right\} \tag{19}$$

and

$$\Delta\hat{\delta}_{n,(i)} = \frac{N}{2\pi n}\mathrm{Arg}\left\{e^{-j2\pi n\hat{\delta}_{(i-1)}/N} r_n \left(\boldsymbol{a}_n^T \boldsymbol{\mu}_{h|r}\right)^*\right\}. \quad (20)$$

Recall that r_0 contains no CFO, so we set $\Delta\hat{\delta}_{0,(i)} = 0$.

3.4 Proposed BLASTS Algorithm

Reorganizing the order of (5)–(8) and (17)–(20), along with the incorporation of the subscript (i) representing the ith iteration, we obtain the BLASTS algorithm, given by

$$\boldsymbol{C}_{h|r,(i)} = \rho_{(i-1)}\left[\boldsymbol{C}_{h,(i-1)}^{-1}\rho_{(i-1)} + \boldsymbol{A}^H\boldsymbol{A}\right]^{-1}, \quad (21)$$

$$\boldsymbol{\mu}_{h|r,(i)} = \left[\boldsymbol{C}_{h,(i-1)}^{-1}\rho_{(i-1)} + \boldsymbol{A}^H\boldsymbol{A}\right]^{-1}\boldsymbol{A}^H\boldsymbol{D}_{\hat{\delta}_{(i-1)}}^H\boldsymbol{r}, \quad (22)$$

$$\rho_{(i)} = \frac{1}{N}\left[|\boldsymbol{r}|^2 - 2\boldsymbol{r}^H\boldsymbol{D}_{\hat{\delta}_{(i-1)}}\boldsymbol{A}\boldsymbol{\mu}_{h|r,(i)} + \mathrm{Tr}\left\{\boldsymbol{A}^H\boldsymbol{A}\left[\boldsymbol{C}_{h|r,(i)} + \boldsymbol{\mu}_{h|r,(i)}\boldsymbol{\mu}_{h|r,(i)}^H\right]\right\}\right], \quad (23)$$

$$\lambda_{l,(i)} = [\boldsymbol{C}_{h|r,(i)}]_{l,l} + \left|[\boldsymbol{\mu}_{h|r,(i)}]_l\right|^2, \quad (24)$$

$$\Delta\hat{\delta}_{(i)} = \frac{\boldsymbol{\mu}_{h|r,(i)}^H\boldsymbol{A}^H\boldsymbol{Q}_N^2\Delta\boldsymbol{\Gamma}_{(i)}\boldsymbol{A}\boldsymbol{\mu}_{h|r,(i)}}{\boldsymbol{\mu}_{h|r,(i)}^H\boldsymbol{A}^H\boldsymbol{Q}_N^2\boldsymbol{A}\boldsymbol{\mu}_{h|r,(i)}}, \quad (25)$$

$$\hat{\delta}_{(i)} = \hat{\delta}_{(i-1)} + \Delta\hat{\delta}_{(i)}, \quad (26)$$

where

$$\Delta\boldsymbol{\Gamma}_{(i)} = \mathrm{Diag}\{\Delta\hat{\delta}_{0,(i)}, \Delta\hat{\delta}_{1,(i)}, \cdots, \Delta\hat{\delta}_{N-1,(i)}\}, \quad (27)$$

$$\Delta\hat{\delta}_{n,(i)} = \frac{N}{2\pi n} \cdot \mathrm{Arg}\left\{e^{-j2\pi n\hat{\delta}_{(i-1)}/N} r_n \left(\boldsymbol{a}_n^T\boldsymbol{\mu}_{h|r,(i)}\right)^*\right\} \quad (28)$$

and $l \in \{0, 1, \cdots, L-1\}$. The initial values are set as $\lambda_{l,(0)} = 1$, $\rho_{(0)} = 0$ and $\hat{\delta}_{(0)} = 0$.

4. Simulation Results and Discussions

Consider $N = 64$ for the OFDM system, and $L = 16$ for the maximum CIR length. Two channels, called Channel A and Channel B, are adopted for the computer simulations. The Channel A model is fixed and the Channel B model is Rayleigh fading. Both the channels have the same non-zero power delay profile $\{\lambda_l = \alpha e^{-l/4}, l = 0, 1, \cdots, 7\}$, where α is for the power control. Therefore, both the channel sparsity ratios are 0.5. For the Channel A model, the lth non-zero channel tap weight is $e^{-l/8}/\sqrt{\sum_{m=0}^{7} e^{-m/4}}$ when we set the total channel power to 1. The preamble is set to be the Zadoff-Chu sequence $\left\{X_n = e^{\frac{j\pi 7n^2}{N}}, n = 0, 1, \cdots, 63\right\}$ [18], [19]. The Zadoff-Chu sequence with the constant amplitude and zero auto-correlation waveform is optimal for the ML CIR estimation [20]. For all the simulation results, the CRB curves [9], [10] are also provided for comparison.

Form Fig. 1, the CFO MSE curve of the STS-ML [10] overlaps with that of the CRB. In addition, the CFO MSE values of the BLAE [16] are smaller than the CRB values when the CFO values are between −0.025 and 0.025. However, the CFO MSE values of the BLAE grow rapidly when the CFO values go further away from zero, showing small CFO estimation range. Noticeably, our proposed BLASTS keeps all the way the lowest CFO MSE values among them, showing the best CFO MSE performance and the wide CFO estimation range. The only short overlap between the BLASTS and the BLAE occurs only when the CFO values are between −0.01 and 0.01.

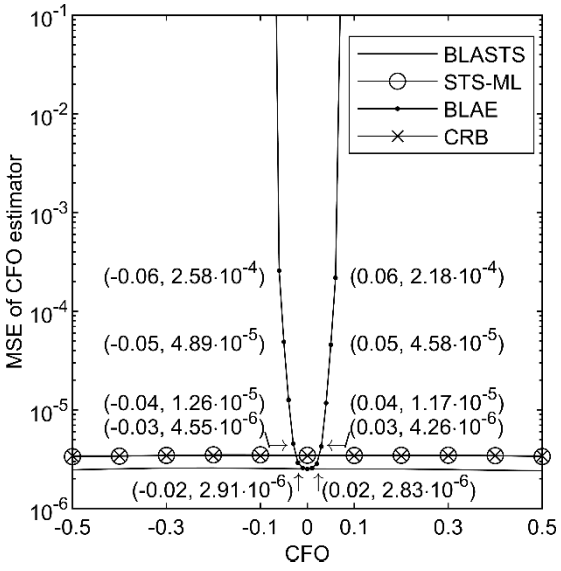

Fig. 1 CFO estimator MSE versus CFO for various algorithms at 30 dB SNR for Channel A.

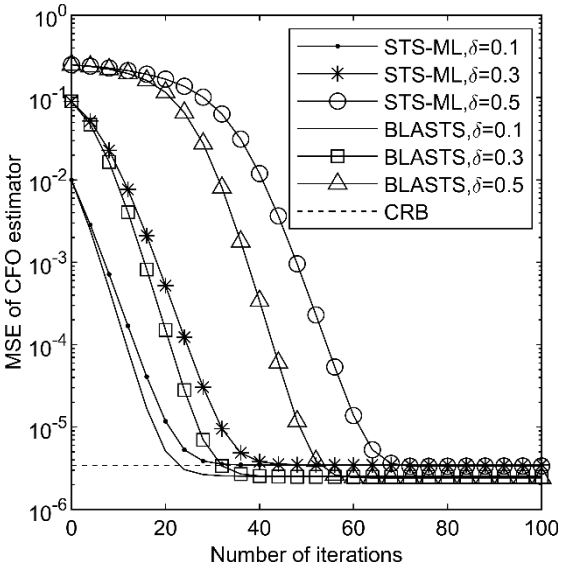

Fig. 2 Learning curve comparison for the STS-ML and the proposed BLASTS at 30 dB SNR for Channel A.

From Fig. 2, the proposed BLASTS shows the faster convergence speeds than the STS-ML does at the same CFO values. Furthermore, the steady-state MSE curves of the STS-ML approach to the CRB curve whereas those of the proposed BLASTS all converge below the CRB curve.

Let us assume that a total of S iterations are needed for

Table 1 Computational complexity.

	STS-ML	BLASTS
real multiplication	$S(8NL+21N+L+7)$	$S(8NL+21N+14L-8)+2N+1$
real division	S	$S(L+1)$
real addition	$S(4NL-2L-1)$	$S(4NL+3L-1)+N-1$
Exp ( )	SL	SL
Arg ( )	$S(N-1)$	$S(N-1)$

Table 2 Complexity comparisons with CFO = 0.5.

	STS-ML	BLASTS
real multiplication	650,012	555,993
real division	68	969
real addition	276,284	236,214
Exp ( )	1,088	912
Arg ( )	4,284	3,591

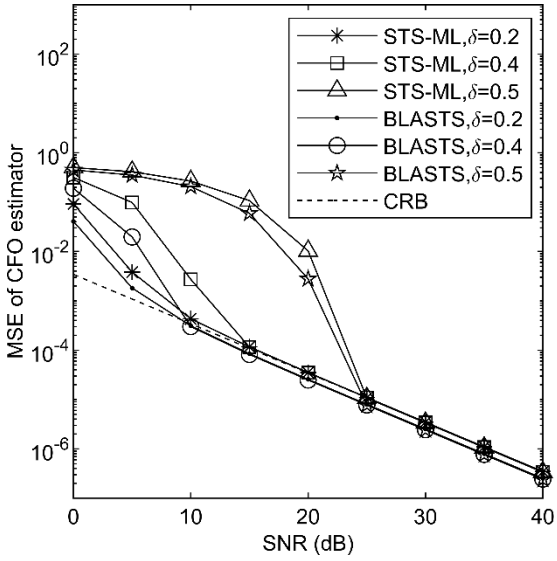

Fig. 3 CFO estimator MSE comparison for the STS-ML and the proposed BLASTS for Channel A.

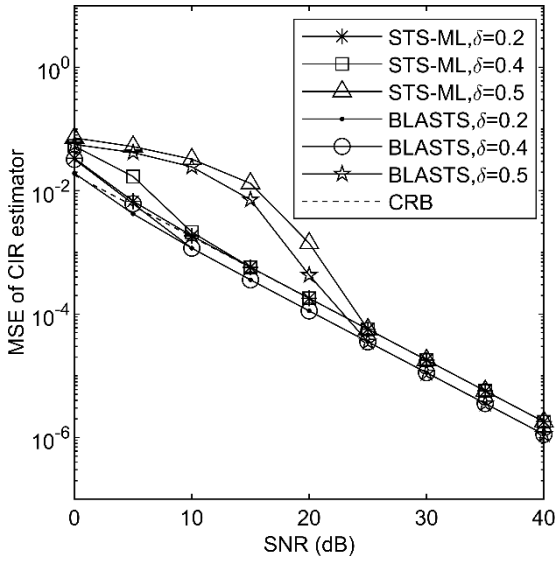

Fig. 4 CIR estimator MSE comparison for the STS-ML and the proposed BLASTS for Channel A.

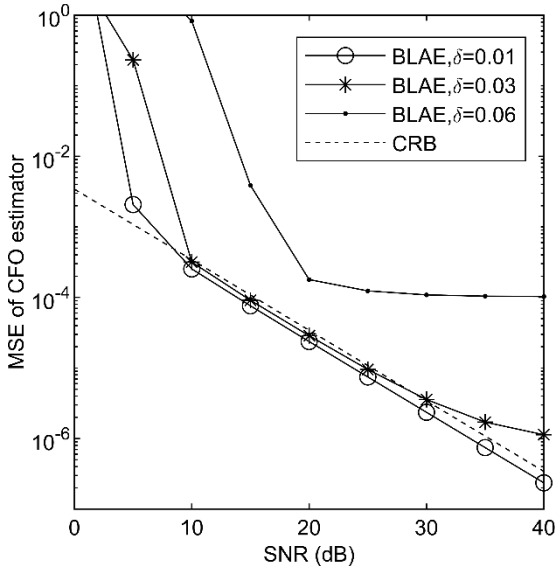

Fig. 5 CFO estimator MSE performance of the BLAE for Channel A.

achieving the steady-state MSE of a learning curve. Then, the various mathematical operation numbers for the STS-ML and the BLASTS are listed in Table 1, where Exp( ) stands for the natural exponential function. Consider the case of δ equal to 0.5. Then, from Fig. 2, the number of S is 57 for the BLASTS while that of S is 68 for the STS-ML. The numbers for the various mathematical operations are list and compared in Table 2. We notice that only the number of the division operation required for the BLASTS is larger than that required for the STS-ML. For all the other kinds of mathematical operations, the STS-ML is much more computationally expensive than the BLASTS. However, the assessment on the overall complexity required for each of the two algorithms is out of the scope of this paper.

For the CFO estimator MSE vs. SNR in Fig. 3, the proposed BLASTS shows the smaller MSE values than the STS-ML does. The similar results for the CIR estimator MSE values of the two algorithms are shown in Fig. 4.

In Fig. 5, the Bayesian learning assisted BLAE [16] algorithm displays the MSE values smaller than the CRB values for $\delta = 0.01$. However, its MSE values increase as the CFO values grow. When the CFO is set at 0.06, its MSE curve greatly departs away from the CRB curve. On the contrary, as having been shown in Fig. 3, both the BLASTS and the STS-ML perform well even though the CFO values go up to 0.5.

Finally, in Figs. 6 and 7, we demonstrate the results of applying the BLASTS and the STS-ML to Channel B,

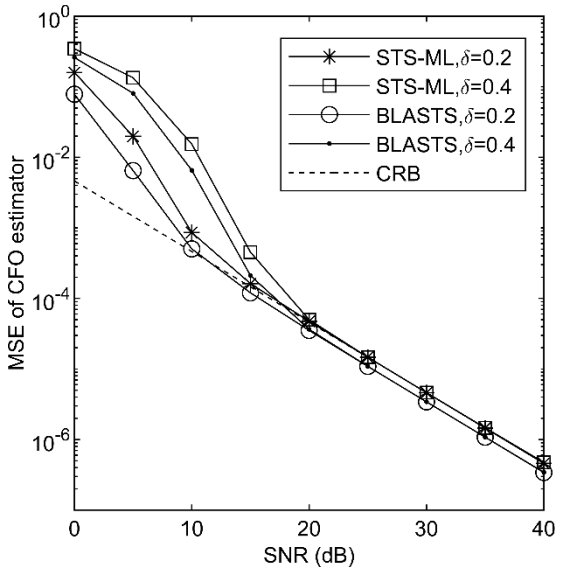

Fig. 6 CFO estimator MSE comparison for the STS-ML and the proposed BLASTS for Channel B.

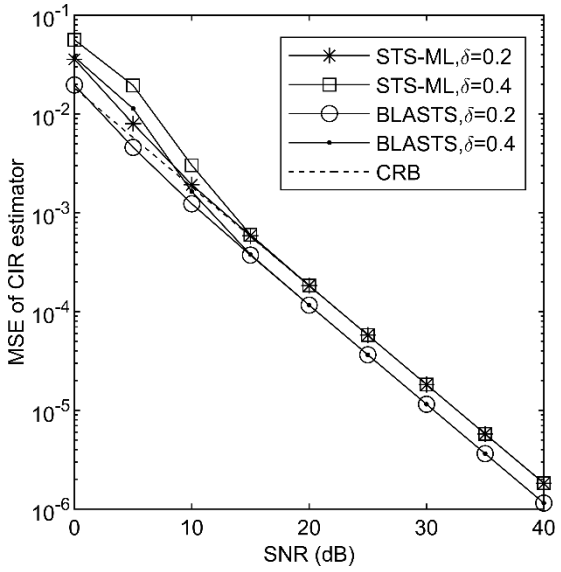

Fig. 7 CIR estimator MSE comparison for the STS-ML and the proposed BLASTS for Channel B.

i.e., the Rayleigh fading channel model. Once again, the BLASTS shows the better MSE performance than the STS-ML does.

5. Conclusions

The BLAE algorithm can achieve the MSE values lower than the CRB values. However, it happens only at small CFO values between −0.025 and 0.025. In addition, the conventional STS-ML algorithm has the wide CFO estimation range from −0.5 to +0.5, and its MSE performance can achieve the CRB. In this paper, we replace the CFO estimator in the BLAE with the STS CFO estimator in the STS-ML. Furthermore, the incorporated STS CFO estimator is redesigned by the EM-based method instead of the original ML-based method. The proposed BLASTS algorithm inherits the low MSE property from the BLAE and the wide CFO estimation property from the STS-ML. At the same time, the convergence speeds of the learning curves have also been improved as compared with those of the STS-ML. These results have been demonstrated by the computer simulations considering a fixed and a Rayleigh frequency-selective channels.

References

[1] T. Pollet, M.V. Bladel, and M. Moeneclaey, "BER sensitivity of OFDM systems to carrier frequency offset and wiener phase noise," IEEE Trans. Commun., vol.43, no.2/3/4, pp.191–193, Feb./March/April 1995. DOI: 10.1109/26.380034

[2] M. Morelli, C.-C.J. Kuo, and M.-O. Pun, "Synchronization techniques for orthogonal frequency division multiple access (OFDMA): A tutorial review," Proc. IEEE, vol.95, no.7, pp.1394–1427, July 2007. DOI: 10.1109/JPROC.2007.897979

[3] A.A. Nasir, S. Durrani, H. Mehrpouyan, S.D. Blostein, and R.A. Kennedy, "Timing and carrier synchronization in wireless communication systems: A survey and classification of research in the last five years," EURASIP J. Wireless Com. Network., vol.2016, no.180, pp.1–38, Aug. 2016. DOI: 10.1186/s13638-016-0670-9

[4] A. Mohammadian and C. Tellambura, "RF impairments in wireless transceivers: Phase noise, CFO, and IQ imbalance — A survey," IEEE Access, vol.9, pp.111718–111791, Aug. 2021. DOI: 10.1109/ACCESS.2021.3101845

[5] X. Ma, H. Kobayashi, and S.C. Schwartz, "Joint frequency offset and channel estimation for OFDM," Proc. IEEE GLOBECOM 2003, vol.1, pp.15–19, Dec., 2003. DOI: 10.1109/GLOCOM.2003.1258193

[6] F.Z. Merli and G.M. Vitetta, "Iterative ML-based estimation of carrier frequency offset, channel impulse response and data in OFDM transmission," IEEE Trans. Commun., vol.56, no.3, pp.497–506, March 2008. DOI: 10.1109/TCOMM.2008.060023.

[7] R.Y. Yen, H.-Y. Liu, and C.-S. Tsai, "Iterative joint frequency offset and channel estimation for OFDM systems using first and second order approximation algorithms," EURASIP J. Wireless Com. Network., vol.2012, no.341, pp.1–10, Nov. 2012. DOI: 10.1186/1687-1499-2012-341

[8] Y. Liu, Z. Tan, H. Wang, and K.S. Kwak, "Joint estimation of channel impulse response and carrier frequency offset for OFDM systems," IEEE Trans. Veh. Technol., vol.60, no.9, pp.4645–4650, Nov. 2011. DOI: 10.1109/TVT.2011.2173362

[9] R.Y. Yen, H.-Y. Liu, and C.-S. Tsai, "Finite high order approximation algorithm for joint frequency tracking and channel estimation in OFDM systems," IEICE Trans. Fundamentals, vol.E95-A, no.10, pp.1676–1682, Oct. 2012. DOI: 10.1587/transfun.E95.A.1676

[10] H.-Y. Liu and R.Y. Yen, "Effective adaptive iteration algorithm for frequency tracking and channel estimation in OFDM systems," IEEE Trans. Veh. Technol., vol.59, no.4, pp.2093–2097, May 2010. DOI: 10.1109/TVT.2010.2042738

[11] S.M. Kay, Fundamentals of Statistical Signal Processing: Estimation Theory, Prentice-Hall, New Jersey, 1993.

[12] M.K. Ozdemir and H. Arslan, "Channel estimation for wireless OFDM systems," IEEE Commun. Surveys Tuts., vol.9, no.2, pp.18–48, July 2007. DOI: 10.1109/COMST.2007.382406

[13] S. Salari, M. Ardebilipour, M. Ahmadian, V. Meghdadi, and J.P. Cances, "EM-based joint ML estimation of carrier frequency offset and channel coefficients in MIMO-OFDM systems," Proc. IEEE PIMRC 2007, Athens, Greece, pp.1–5, Sept. 2007. DOI: 10.1109/PIMRC.2007.4394414

[14] M.-O. Pun, M. Morelli, and C.-C.J. Kuo, "Iterative detection and frequency synchronization for OFDMA uplink transmissions," IEEE Trans Wireless Commun., vol.6, no.2, pp.629–639, Feb. 2007. DOI: 10.1109/TWC.2007.05368

[15] J.H. Lee, J.C. Han, and S.C. Kim, "Joint carrier frequency synchronization and channel estimation for OFDM systems via the EM algorithm," IEEE Trans. Veh. Technol., vol.55, no.1, pp.167–172, Jan. 2006. DOI: 10.1109/TVT.2005.861212

[16] S. Salari and F. Chan, "Joint CFO and channel estimation in OFDM systems using sparse Bayesian learning," IEEE Commun. Lett., vol.25, no.1, pp.166–170, Jan. 2021. DOI: 10.1109/LCOMM.2020.3024817

[17] S. Haykin, Adaptive Filter Theory, 4th ed., Prentice-Hall, New Jersey, 2002.

[18] R.L. Frank, S.A. Zadoff, and R.C. Heimiller, "Phase shift pulse codes with good periodic correlation properties," IRE Trans. Inf. Theory, vol.8, no.6, pp.381–382, Oct. 1962. DOI: 10.1109/TIT.1962.1057786

[19] D.C. Chu, "Polyphase codes with good periodic correlation properties," IEEE Trans. Inf. Theory, vol.18, no.4, pp.531–532, July 1972. DOI: 10.1109/TIT.1972.1054840

[20] H. Minn and N. Al-Dhahir, "Optimal training signals for MIMO OFDM channel estimation," IEEE Trans Wireless Commun., vol.5, no.5, pp.1158–1168, May 2006. DOI: 10.1109/TWC.2006.1633369

Hong-Yu Liu received the M.S. degree from National Cheng Kung University, Tainan, Taiwan in 1994, and the Ph.D. degree from Tamkang University, Taipei, Taiwan in 2006, all in electrical engineering. He joined the faculty of the department of computer and communication engineering at Dahan Institute of Technology in 1998. He was with the Fu Jen Catholic University, Taipei, Taiwan, in 2011 where he is currently as an associate professor of Electrical Engineering. His research interests lie in the area of OFDM synchronization, multi-channel detection and estimation, and space-time coding. Dr. Liu was elected as an honorary member of the Phi Tau Phi Scholastic Honor Society of the Republic of China in 2006.